Functional Materials 13, No.3 (2006)

Electronic structure of Ni–Mn–Ga magnetic shape memory alloy studied by EELS method

R.Ochoa-Gamboa, H.Flores-Zuniga, F.Espinosa-Magana, D.Rios-Jara, I.Glavatskyy, N.Glavatska**

Centro de Investigacion en Materiales Avanzados S.C.,
Miguel de Cervantes #120, 31109, Chihuahua, Chih, Mexico
*G.Kurdyumov Institute for Metal Physics, Department of Alloyed Steels,
National Academy of Sciences of Ukraine,
36 Vernadsky blvd., 03142, Kyiv, Ukraine

The evolution of *3d* electronic structure associated with the martensitic transformation and ferromagnetic transition in non-stoichiometric Ni_2MnGa alloy possessing the shape magnetic memory were studied by electron-energy loss spectroscopy (EELS) and with theoretical modeling methods. The EELS spectra of Ni-Mn-Ga crystals have been obtained under *in-situ* heating to study the electron structure of ferromagnetic (FM) martensite, FM austenite and paramagnetic austenite. When considering the EELS spectra, the total white lines intensity $L_{23} = L_2 + L_3$ as well as as well as the L_3/L_2 ratio and conclusions have been drawn on the occupancy of the 3*d* state fromAs L_{23} reflects the unoccupied density of states in *3d* bands, these results indicate that no charge transfer has taken place during martensitic transformation and changes in the magnetic dipole moments at phase transitions. The experimental results have shown that the magnetic dipole moment on Ni atoms decreases at the reverse martensitic transformationwhile it increases on Mn, and the charge is observed to be redistributed between Mn и Ni in agreement with *ab-initio* numerical calculations.

Исследована эволюция *3d* электронной структуры нестехиометрического сплава Ni–Mn–Ga, обладающего эффектом магнитной памяти формы, методом электронной спектроскопии энергетических потерь (EELS) и теоретического моделирования. EELS спектры монокристаллов Ni–Mn–Ga получены при нагреве *in-situ* для изучения электронной структуры ферромагнитной мартенситной, ферромагнитной аустенитной и парамагнитной аустенитной фаз. При анализе EELS спектров определены соотношения белых линий L_3/L_2 и полная интенсивность $L_{23} = L_2 + L_3$, сделан вывод относительно заполнения *3d* состояния и изменения магнитных дипольных моментов при фазовых переходах. Экспериментальные результаты показывают, что при обратном мартенситном превращении магнитный дипольный момент на атомах Ni уменьшается, в то время как для атомов Mn — увеличивается и наблюдается перераспределение заряда между атомами Mn и Ni, что согласуется с проведенными в работе *ab-initio* вычислениями.

Ferromagnetic shape memory alloys have attracted increased attention because of large magnetically induced strain. Ni–Mn–Ga Heusler alloys undergo reversible ferromagnetic and martensitic transformations, on cooling from paramagnetic (PM) austenite to ferromagnetic (FM) austenite and thereafter to FM martensite. Very few works on the electronic characteristics of these phase transitions have been reported in the literature, although we could expect electronic phenomena should play an important role given the magnetic properties involved. In this work we study changes in

electronic structure of a non-stoichiometric Ni_2MnGa alloy by using electron energy loss spectroscopy (EELS) and electronic structure calculations with the spin-polarized variant of LAPW calculations method performed using Wien2k package.

Electron energy-loss spectroscopy is a powerful analytical technique that can be utilized to obtain information on the structure, bonding and electronic properties of a material [1–7]. The interactions of fast electrons with the specimen result in excitations of electrons into unoccupied energy levels in the conduction band as well as collective excitations of valence electrons. When a spectrum is obtained by analyzing the energy lost by the incident electrons, the region up to an energy loss of ~50 eV is dominated by collective excitations of valence electrons (plasmon) and by interband transitions. At higher energy losses ionization edges occur due to excitation of core electrons of the constituent atoms into the conduction band.

The excitation of atomic inner shells by high-energy electrons provides a method for studying the unoccupied conduction states in a solid. These core-level processes are mostly sensitive to final states since the initial states have narrow energy widths. Besides the well defined ionization edges there is a fine structure superposed on the edge and extending up to about 50 eV from the edge onset, which is associated with the density of unoccupied states in the conduction band, known as the energy loss near edge structure (ELNES).

In case of the *3d* transition metals and their alloys, L_{23} edges of EELS are characterized by two sharp peaks, known as "white lines". Because the predominance of dipole transitions, these white lines originate from excitations of $2p_{1/2}$ and $2p_{3/2}$ core electrons to unoccupied *d*-like states near the Fermi level. The white-lines intensities reflect the unoccupied *3d* density of states (DOS). The data on the occupancies of the *3d* and *4d* states [8–16] may clarify many issues fundamental to the electronic theories of transition metal alloys, including phase transformations. Pearson et al. [8] have attempted to relate the sum of the L_3 and L_2 white-lines intensities to the occupancies of the corresponding outer *d* states. The experimental studies on the white lines from L_{23} EELS spectra for elemental metals of the *3d* transition series show that the normalized intensities of these white lines decreased nearly linearly with increasing *d*-state occupancy across the series. The normalized white-line intensity was defined as the integrated intensity of the L_2 and L_3 white lines divided by the integrated intensity in a normalization window 50 eV in width beginning 50 eV past the L_3 edge onset. When the normalized white-line intensities for the *3d* metals were divided by appropriate matrix-element correction factors, which were calculated for each atomic species, a linear correlation with *3d* occupancy was obtained with a fit given by

$$I_{3d} = 10.8\,(1 - 0.1 n_{3d}), \qquad (1)$$

where I'_{3d} is the normalized white-line intensity divided by the appropriate matrix-element correction factor and n_{3d} is the *3d* occupancy in electron/atom. The above correlation between the normalized white-line intensity and *3d* occupancy (electrons/atom) is useful for determining changes in outer *d* state occupancy upon alloying and solid-state phase transformations if the corresponding changes in the normalized white-line intensity are observed.

On the other hand the ratio L_3/L_2 that would be expected to be 2.0 because the occupation number of the state is $2j + 1$, where j is the total angular momentum quantum number and for *p* states $j = 1/2$, $3/2$, deviates from the statistical ratio because the ejected electron creates a core-hole which splits the final states into two groups with a large energy separation due to the spin-orbit interaction. Experimental measurements have shown a wide range of variation in L_3/L_2 and it is not linearly related to the density of unoccupied *3d* states. In order to explain the deviations from the statistical ratio, a full atomic approach, including crystal and spin-orbit coupling will be necessary. Nevertheless since the L_2 and L_3 edges are related to the spin-orbit coupling of *3d* electrons, the intensity ratio of the white lines is related not only to the distribution of the *d* electrons buy also to the magnetic moment of the atoms (e.g. their spin states) [21, 22]. Higher L_3/L_2 is believed to indicate a higher local magnetic moment of the atom as this ratio is approximately the ratio of holes in the $j = 5/2$ to $j = 3/2$ in the final *3d* states.

Electronic structure calculation is carried out with the modeling method using the program WIEN2k [7] in LAPW approach with local spin density approximation (LSDA). All modeling calculations were made

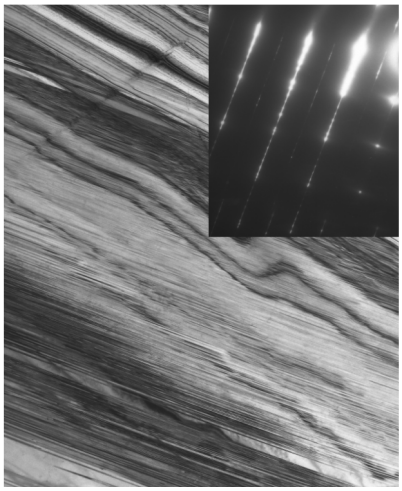

Fig. 1. Micrograph and diffraction pattern from martensite at room temperature.

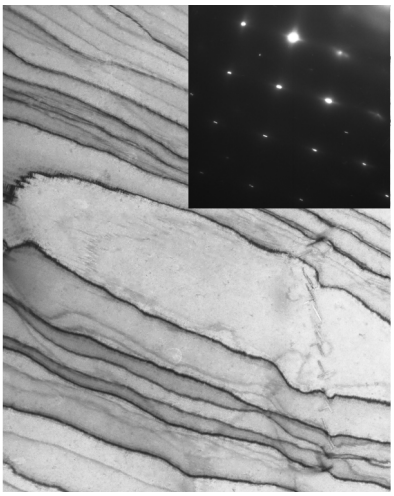

Fig. 2. Micrograph and diffraction pattern from ferromagnetic austenite at 60°C.

ignoring non-stoichiometric deviations of the real studied composition using Ni_2MnGa approximation. The electronic structure of valence and condiction band, distribution of total and partial atomic densities, energy band structure $E(k)$, charge and spin states of atoms, total and partial electron densities on Fermi level are investigated. As the modern computing program WIEN 2k used for calculation and modeling of an electronic structure can not calculate real 5M structure, we use the approximation of real 5M modulated structure by BCT unit cell as it is conventional for that type of calculations in the literature.

The non-stoichiometric $Ni_{48.54}Mn_{27.12}Ga_{24.34}$ (in at.%) single crystal was grown from single crystalline ingot using Bridgman method, with following homogenization (72 h at 1273 K) and annealing for ordering (48 h at 1070 K) sealed in quartz ampoules in protective Ar atmosphere. The single crystal $10\times10\times7$ mm^3 was cut to have faces parallel to {100} of FCC austenite, then grounded and electro-polished. The martensitic transition and Curie point temperatures (M_S = 311 K and T_C = 378 K, respectively) were determined by low-field magnetic susceptibility method. The crystal structure and lattice parameters of the austenite and martensite phases were studied using 3-circle X-ray diffractometer with CuK_α radiation.

The martensite lattice was determined as BCT with 5-layered packing modulation. Ignoring, for simplicity, the 5M superstructure of the martensite, we use BCT approximation with lattice parameters at 290 K: a = 4.22 Å, c = 5.57 Å; and for the FCC austenite (T = 333 K): a = 5.84 Å.

Electron energy loss spectra were obtained during in-situ heating at 293, 333 and 393 K in order to acquire spectra from FM martensite, FM austenite and PM austenite, using Gatan parallel electron energy loss spectrometer (PEELS model 766) attached to a Philips CM-200 transmission electron microscope (TEM). Spectra were taken in diffraction mode with 0.3 eV/ch dispersion, an aperture of 3 mm and a collection semi-angle of 2.7 mrad. The resolution of the spectra was determined by measuring the full width at half-maximum (FWHM) of the zero-loss peak and this was typically close to 1.8 eV, when the TEM was operated at 200 kV. The EELS spectra were corrected for dark current and readout noise. The channel to channel gain variation was minimized by normalizing the experimental spectrum with independently obtained gain spectrum of the spectrometer. All spectra were examined for oxygen edges to prevent any surface oxides.

Spectra in the high-energy region were background-subtracted by fitting the pre-edge backgrounds with a power-law function and then Fourier-Ratio deconvoluted to remove multiple scattering components from the spectra.

Figs. 1,2 show micrographs and diffraction patterns of the alloy at 293 K (FM martensite) and 333 K (FM austenite). It is clearly observed, from twin boundaries in the bright field micrograph and streaks in the diffraction pattern, that a martensitic transformation has taken place.

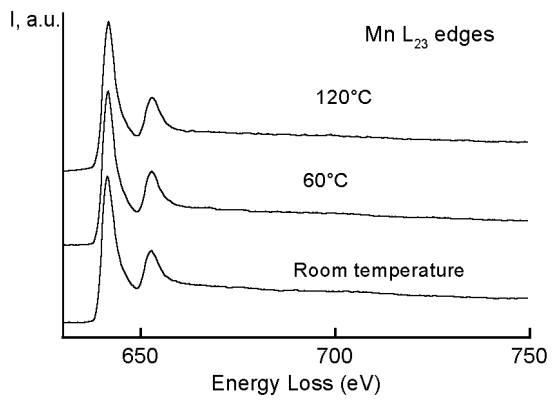

Fig. 3. Superposition of Mn L_{23} edges from paramagnetic austenite (293 K), ferromagnetic austenite (333 K) and ferromagnetic martensite at room temperature.

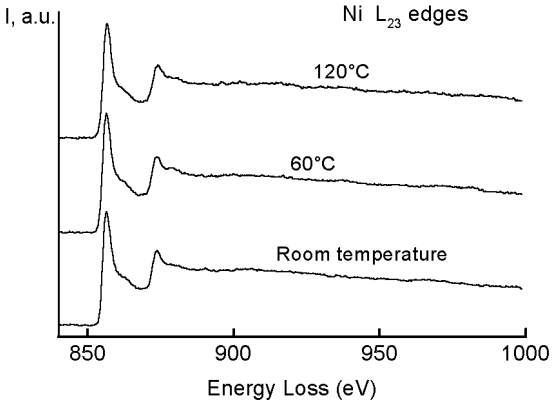

Fig. 4. Superposition of Ni L_{23} edges from paramagnetic austenite (120°C), ferromagnetic austenite (60°C) and ferromagnetic martensite at room temperature.

Energy-loss spectra for Mn and Ni L_{23} ionization edges are shown in Fig. 3 and Fig. 4, respectively, for FM martensite (293 K), FM austenite (333 K) and PM austenite (393 K), where spectra were shifted up for clarity.

At the first sight, no changes are observed in fine structure (ELNES), which reflects the density of states (DOS) at Mn and Ni sites. Furthermore, as EELS probes the symmetry-projected DOS, the ELNES in this case must be directly compared to *d*-symmetry DOS, because of the predominance of transitions from *2p* to *3d* states. Electronic structure calculations performed with the LAPW method (Wien2k code) shows a strong hybridization between Mn and Ni *d*-orbitals. However, the fine structure obtained from numerical calculations is smoothed in EELS spectra due to our experimental resolution ~ 1.8 eV.

On the other hand, the occupancy and distribution of *3d* electrons are obtained from the total intensity L_{23} and the ratio L_3/L_2 of the white lines. To extract the white-lines we closely follow the empirical method developed by Pearson et al. [10], by modeling the background with a double step function, with steps at L_2 and L_3 peaks. A step line was fit to the background immediately following the L_2 white line. This line was then modified into a double step of the same slope with onsets occurring at the white lines maxima. The ratio of the step heights was chosen as 2:1 which is the multiplicity of the initial steps (four $2p_{3/2}$ electrons and two $2p_{1/2}$ electrons). The white lines areas was then divided by the area in a normalization window 50 eV in width, beginning 50 eV past the onset of the L_3 white line, which yields a normalized white-line intensity for the alloy. Dividing by the matrix-element factor, 0.129 for Mn and 0.169 for Ni, and using Eq.(1) allows us to obtain Δn_{3d} in electron/atom for the transitions. Table 1 shows the results obtained for PM austenite, FM austenite and FM martensite phases after isolation of the white lines, with values for the white lines ratio L_3/L_2, normalized white lines intensities L_{23} and occupation number (n_{3d} — electrons/atom in *3d* states) for Mn and Ni.

From these results we conclude that no charge transfer seems to take place during martensitic transformation nor in the ferromagnetic transition as these values should imply maximum transfers of ~0.05 electrons/atom, which is within the experimental accuracy (0.06 electrons/atom). On the other hand, the ratio L_3/L_2, which is related to the magnetic dipole moment per atom, shows a clear tendency, during the reverse martensitic transformation, from martensite to austenite, the white lines ratio increases for Mn and decreases for Ni, implying the magnetic dipole moment increases for Mn and decreases for Ni, which is in qualitative agreement with numerical

Table 1. Results of the experimental EELS studies of the Ni–Mn–Ga single crystal

T(K)	L_3/L_2		L_{23}		n_{3d}	
	Mn	Ni	Mn	Ni	Mn	Ni
393 (PM austenite)	3.02	3.26	0.50	0.19	6.41	8.96
333 (FM austenite)	2.91	3.29	0.53	0.19	6.20	8.96
293 (FM martensite)	2.79	3.37	0.52	0.18	6.27	9.01

Table 2. Magnetic moments of individual atoms and unit cell in FCC and BCT modifications

FCC austenite		BCT martensite	
Atom	Magnetic moment, μ_B	Atom	Magnetic moment, μ_B
Mn	3.46	Mn	3.43
Ni	0.35	Ni	0.39
Ga	−0.05	Ga	−0.05
Unit cell	4.14	Unit cell	4.19

calculations as shown in Table 2. The same trend is observed during ferromagnetic transition even though we could not find a reference to compare with. In a near future we will carry out experiments for measuring the magnetic dipole moment at the three phases in order to correlate it with values of white lines ratios and will published elsewhere.

Changes in the electronic structure during the martensitic transformation and ferromagnetic transition in a Ni–Mn–Ga alloy were studied by electron energy loss spectroscopy and numerical calculations. From EELS, we analyzed the changes in Ni and Mn L_{23} white-lines intensity before and after the transformation, as well as the ratio L_3/L_2. It was found that no charge transfer occurred during the martensitic transformation or ferromagnetic transition, but a redistribution of electrons in *3d* bands, changing the magnetic dipole moment per atom, as predicted by numerical calculations.

Valence band of the studied Ni–Mn–Ga alloy martensite phase consists of two subbands. The first, pre-Fermi, is situated till ~10 eV deeply from Fermi level for FCC- and ~7 eV for BCT-modification. The second, narrow band of deep states has binding energy near −14...−16 eV and formed by gallium *3d*-electrons. Pre-Fermi band is mainly formed by hybridized states of nickel and manganese atoms. Ni*3d*-electrons dominate on Fermi level.

Large splitting of Ni and Mn states testifies to their significant interactions, while those of Ga atoms with other alloy components are weakened. Dispersion laws are quite different for electrons with different spin directions.

As a result of transition from austenite to martensite the magnetic moment of nickel atoms increases by $0.04\mu_B$ and the magnetic moment of manganese atoms decreases by $0.03\mu_B$. As a consequence, the magnetic moment of whole cell rises by $0.05\mu_B$.

References

1. R.F.Egerton, in: Electron Energy Loss Spectroscopy in the Electron Microscope, 2nd Edition, Plenum Press, New York (1996).
2. M.M.Disko, C.C.Ahn, B.Fultz (eds.), Transmission Electron Energy Loss Spectrometry in Materials Science, The Minerals, Metals and Materials Society, Warrendale, Pennsylvania (1992).
3. G.Soto, E.C.Samano, R.Machorro et al., *Appl. Surf. Sci.*, **183**, 246 (2001).
4. K.van Benthem, C.Elsässer, *J.Appl. Phys.*, **90**, 6156 (2001).
5. K.van Benthem, R.H.French, W.Sigle et al., *Ultramicroscopy*, **86**, 303 (2001).
6. G.Brockt, H.Lakner, *Micron*, **31**, 435 (2000).
7. S.M.Bose, *Phys. Rev. Lett. A*, **289**, 255 (2001).
8. D.H.Pearson, B.Fultz, C.C.Ahn, *Appl. Phys. Lett.*, **53**, 1405 (1988).
9. D.H.Pearson, C.C.Ahn, B.Fultz, *Phys. Rev. B*, **47**, 8471 (1993).
10. D.H.Pearson, C.C.Ahn, B.Fultz, *Phys. Rev. B*, **50**, 12969 (1994).
11. G.Y.Yang, Jing Zhu, *J. . Magn. Magn. Mater.*, **220**, 65 (2000).
12. P.L.Potapov, S.E.Kulkova, D.Schryvers, J.Verbeeck, *Phys. Rev. B*, **64**, 184110 (2001).
13. G.A.Botton, G.Y.Guo, W.M.Temnerman, C.J.Humphreys, *Phys. Rev. B*, **54**, 1682 (1996).
14. Yasukazu Murakami, Daisuke Shindo, Kazuhiro Otsuka, Tetsuo Oikawa, *J. Electron Microsc.*, **47**, 301 (1998).
15. R.D.Leapman, L.A.Grunes, P.L.Fejes, *Phys. Rev. B*, **26**, 614 (1982).
16. T.G.Sparrow, B.G.Williams, C.N.R.Rao, J.M.Thomas, *Chem. Phys. Lett.*, **108**, 547 (1984).
21. G.A.Botton, C.C.Appel, A.Horsewell, W.M.Stobbs, *J. Microsc.*, **180**, 211 (1995).
22. S.J.Lloyd, G.A.Botton, W.M.Stobbs, *J. Microsc.*, **180**, 288 (1995).

EELS дослідження електронної структури сплаву Ni–Mn–Ga з ефектом магнітної пам'яті форми

Р.Очоа-Гамбоа, Г.Флорес-Зунига, Ф.Эспиноза-Магана, Д.Риос-Яра, І.Главацький, Н.Главацька

Досліджено еволюцію *3d* електронної будови нестехіометричного сплаву Ni–Mn–Ga, який виявляє ефект магнітної пам'яті форми, методом електронної спектроскопії енергетичних втрат (EELS) та теоретичного моделювання. EELS спектри монокристалів Ni–Mn–Ga отримано при нгаріванні *in-situ* для вивчення електронної будови феромагнітної мартенситної, феромагнітної аустенітної та парамагнітної аустенітної фаз. При аналізы EELS спектрів визначено співвідношення білих ліній L_3/L_2 та інтегральна інтенсивність $L_{23} = L_2 + L_3$, зроблено висновки щодо заповнення *3d* стану та змін магнітних дипольних моментів при фазових перетвореннях. Експериментальні результати свідчать, що при зворотному мартенситному перетворенні магнітний дипольний момент на атомах Ni зменшується, а на атомах Mn збільшується, також спостерігається перерозподіл заряду між атомами Mn и Ni, що узгоджується із проведеними у роботі *ab-initio* розрахунками.